J Supercond Nov Magn (2015) 28:1737–1741
DOI 10.1007/s10948-015-3000-2

ORIGINAL PAPER

The Effect of Anisotropy of H_{c2} on Transport Current in Silicone Oil-Doped MgB_2 Superconductor

S. R. Ghorbani · M. Fahimi

Received: 15 December 2014 / Accepted: 23 January 2015 / Published online: 4 February 2015

Abstract The temperature and magnetic field dependences of the critical current density in silicone oil-doped MgB_2 polycrystalline samples have been investigated by magnetic measurements. The upper critical magnetic field anisotropy, $\gamma = H_{c2}^{\perp c}/H_{c2}^{||c}$ dependence of the critical current density, $J_c(B)$, were analyzed within the percolation model. The calculated critical current densities based on percolation theory are in agreement with the experimental data. It was found that the anisotropy, γ, and the percolation threshold parameter, p_c, show different trends in their temperature dependence, where γ increases, but p_c decreases with increasing temperature. It is suggested that the anisotropy is responsible for the reduction of the critical current density in high magnetic field. The relationship between the anisotropy and the volume pinning force is investigated. It was found that the position of the maximum of the volume pinning force is shifted to lower reduced magnetic field by decreasing the anisotropy and increasing the percolation threshold p_c.

Keywords Superconductivity · Doped MgB_2 · Anisotropy · Critical current

1 Introduction

Soon after the discovery of superconductivity in MgB_2 [1], great research efforts were made to improve its properties, such as the critical current density and the upper critical field, that are important for power applications. It was found that grain boundaries do not inhibit the critical current in polycrystalline MgB_2 samples [2, 3]. The critical current rapidly decreases with increasing field, however, becoming zero at the irreversibility field, H_{irr}, which is far below the upper critical field [4]. The current density decay behavior is governed by the pinning mechanism, which is still under investigation. Anisotropy was identified as a possible reason for the field dependence of the critical current density, J_c [5]. The influence of anisotropy on the field dependence of J_c was evaluated in terms of percolation theory [6]. Percolation theory is a model displaying a phase transition that has been employed frequently to analyze currents in granular superconductors [7–15], especially in high-temperature superconductors, HTS. In HTS, grain boundaries limit the current flow. This model was also used to interpret the irreversibility line in MgB_2 superconductor [5]. The polycrystalline MgB_2 samples are assumed to consist of grains with identical properties, except that their *c*-axes are randomly oriented. At a fixed temperature, the upper critical field depends on the angle between the *c*-axis in the grain and the applied magnetic field. It was found that with increasing magnetic field, the grain will soon become a normal conductor [16], thus reducing the effective cross-section of the sample and decreasing the critical current density.

In this work, the influence of anisotropy on the transport current in silicone oil-doped polycrystalline MgB_2 samples and the field dependence of the critical current density in terms of percolation theory are investigated. It was found that the anisotropy, γ and the percolation threshold parameter, p_c, show different trends as functions of temperature, so that γ increases, but p_c decreases with increasing temperature. Results of the volume

S. R. Ghorbani (✉)
Department of Physics, Ferdowsi University of Mashhad, Mashhad, Iran
e-mail: sh.ghorbani@um.ac.ir

M. Fahimi
Department of Physics, Hakim Sabzevari University, Sabzevar, Iran

pinning force analysis show that the volume pinning force depends on the anisotropy and the percolation threshold parameters.

2 Experimental

MgB_2 bulk samples were prepared by the standard solid-state in situ method with 10 % silicone oil (–SiC_2H_6O–)$_n$ addition. Silicone oil was dissolved in acetone, and the obtained solution was mixed with an appropriate amount of boron powder (99 %) and dried in a vacuum oven. The dried mixture was mixed with magnesium powder (99 %). The powder was pressed into cylinders, which were heated from room temperature to 600 and 900 °C under argon atmosphere to reduce the oxidation of the samples, which resulted in samples with critical temperatures of 35.2 and 36.4 K, respectively, which has been well described elsewhere [17].

The crystalline structure was investigated using X-ray diffraction (XRD). It was found that the main impure phase is MgO, as a result of oxygen in the samples, which may have been introduced in the process of pressing. Magnetization measurements were performed in a magnetic properties measurement system (MPMS). The critical current density (J_c) values in full penetration were estimated by using the Bean model: $J_c = 20\Delta M/Va(1-a/3b)$, where $a$and b are the width and the length of the sample perpendicular to the applied field ($a<b$), respectively, V is the sample volume, and ΔM is the height of the M-H hysteresis loop. Magnetization measurements were made on the sample size of 1×2.22×3.52 mm^3. The accuracy of the extracted J_c values based on the Bean model was analyzed along the Johansen and Bratsberg model (JBM) [18].

3 Results and Discussion

Figure 1 shows the magnetic field dependence of the critical current density for two samples sintered at different temperatures. The J_c initially shows a plateau (see Fig. 2) at low field and then begins to decrease quickly as the field increases. Furthermore, J_c decreases even faster with increasing temperature. The accuracy of the extracted J_c values was analyzed along the approach developed by Johansen and Bratsberg (JB) [18]. According to the JB model, the J_c as a function of magnetic field is given by the following expression:

$$J_c(B)=\frac{\Delta M\,(B)}{Va\left(1-\frac{a}{3b}\right)}\left[1-\frac{1}{40}\frac{\left(5-\frac{3a}{b}\right)}{\left(3-\frac{a}{b}\right)}a^2\mu_0^2\frac{d^2}{dB^2}J_c^2(B)+\cdots\right] \tag{1}$$

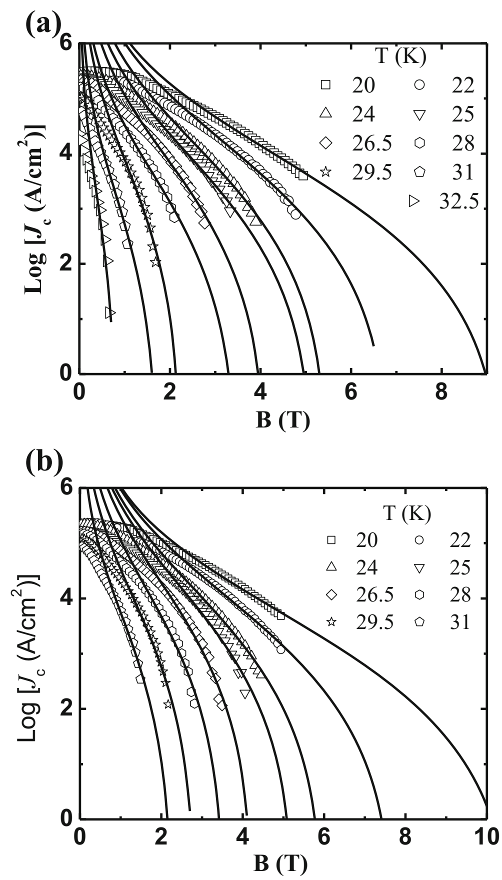

Fig. 1 The critical current density as a function of applied magnetic field at different temperatures for samples sintered at **a** 600 °C and **b** 900 °C. The *solid curves* are calculated by the percolation model

It is clear that the lowest-order correction term in the Bean model is

$$C.T.=\frac{1}{40}\frac{\left(5-\frac{3a}{b}\right)}{\left(3-\frac{a}{b}\right)}a^2\mu_0^2\frac{d^2}{dB^2}J_c^2(B) \tag{2}$$

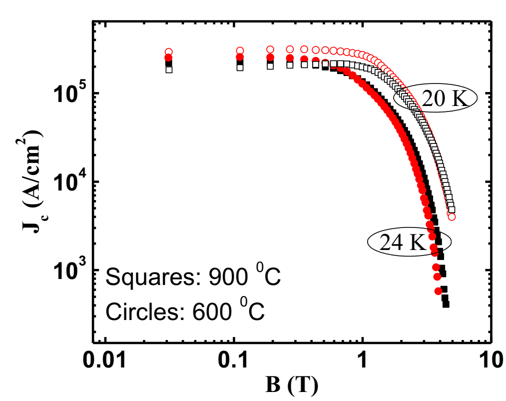

Fig. 2 Comparison of critical current density at temperatures of 20 and 24 K in two samples sintered at 600 and 900 °C

With $a = 1$ mm, $b = 2.22$ mm, $\mu_0 = 4\pi \times 10^{-5}$ T cm/A, and $d^2(J_c^2(B))/dB^2$ of order 8–10 at $B = 1$–5 T for our experimental data, the correction term (C.T.) of Eq. (2) becomes roughly 1/20. Therefore, the extracted J_c values according to the Bean model determine only weakly the contribution of the second term in Eq. (1).

For understanding the effect of sintering temperature on the critical current density, the J_c values of the two samples sintered at 600 and 900 °C are compared in Fig. 2 at temperatures of 20 and 24 K. As can be seen from this figure, the critical current density of the sample sintered at 900 °C is higher at higher magnetic fields than for the sample sintered by the 600 °C reaction. This is in agreement with the increased connectivity resulting from the higher temperature reaction. While at both low magnetic fields and low temperatures, the samples sintered at 600 °C have higher J_c, which is in striking contrast with the decreased connectivity. It was found, however, that the grain size in SiC-doped MgB_2 is significantly smaller after the 600 °C reaction than after the 900 °C [19]. At low magnetic fields, the high J_c data after the 600 °C reaction are consistent with strong vortex pinning by grain boundaries, which have been shown [2] to be important pinning centers in MgB_2.

In order to analyze the critical current density results, the percolation model was used. According to the Ginzburg-Landau theory [2], the upper critical field of each grain depends on the angle between the c-axis in the grain and the applied magnetic field. The upper critical magnetic field, B_{c2}, as function of angle at constant temperature is given by the following expression [22]:

$$B_{c2}(\theta) = \frac{B_{c2}\left(\frac{\pi}{2}\right)}{\sqrt{\mathrm{Sin}(\theta)^2 + (\gamma \mathrm{Cos}(\theta))^2}} \tag{3}$$

where $\gamma = B_{c2}(\frac{\pi}{2})/B_{c2}(0)$ or $= H_{c2}^{\perp c}/H_{c2}^{||c}$ denotes the anisotropy factor of the upper critical field and θ is the angle between the applied field and the c axis.

The conductivity in a granular superconductor becomes a function of the current density J. At a fixed magnetic field, on decreasing the temperature of a polycrystalline sample, some grains will become superconducting and with continuously decreasing temperature, more and more grains become superconductors, depending on their orientation. During this transition, the system consists of both normal and superconducting grains. When a certain fraction of grains becomes superconducting, the first continuous superconducting current occurs. This fraction is defined as the percolation threshold p_c. The percolation model for J_c is based on a percolation crosssection, where the current become $I = \sigma_p J$. σ_p can be interpreted as the total cross-section of all current paths existing at a certain fraction p of conducting particles. If we know the distribution function of the critical current densities within the grains the resulting critical current density can be calculated from the percolation crosssection. Based on percolation theory the Dew-Hughes model of grain boundary pinning [23], and the GinzburgLandau theory, the expression for critical current can be obtained [22]

$$J_c = f_{p0} \frac{\left(1 - \frac{B}{B(\rho=0)}\right)^2}{\sqrt{B \cdot B(\rho = 0)}} A_p \left(\frac{p_{max} + p_c}{2.2}, p_c\right) \tag{4}$$

where f_{p0} shows the pinning strength and $B(\rho = 0)$ represents the zero resistivity field that is proportional to the upper critical magnetic field [24]

$$B(\rho = 0) = \frac{B_{c2}}{\sqrt{\left(\gamma^2 - 1\right) p_c^2 + 1}} \tag{5}$$

$A_p = \sigma_p/\sigma$ denotes the reduced effective percolation crosssection and σ is the sample crosssection. p_c is the minimum fraction of superconducting grains for a continuous superconducting current, and it strongly depends on the number of connections between grains and therefore on the preparation conditions. The p_c increases with a decreasing number of connections between the grains, and thus low connectivity is expected to result in a larger p_c. The expression for A_p (p, p_c) is given by

$$A_p(p, p_c) = \left(\frac{p(J) - p_c}{1 - p_c}\right)^t \tag{6}$$

where t is depends on the dimensionality of the system and it is predicted to be 1.79 in three-dimensional systems p_{max} is the relative fraction of superconducting grains at the applied magnetic field, which refers to the maximum of $p(J)$ [22]

$$p_{max}(B) = p\left(B_{c2}(\theta) \geq B\right) = \sqrt{\frac{\left(\frac{B_{c2}^{ab}}{B}\right)^2 - 1}{\gamma^2 - 1}} \tag{7}$$

Equation (4) was used to analyze the critical current density. As shown in Fig. 1, in the high magnetic field region, the experimental data are well fitted to Eq. (4), but there is a deviation from the percolation model at low magnetic fields. This is because at low fields, i.e. $B/B(\rho = 0) \to 0$, Eq. (4) leads to the proportionality of $J_c \propto 1/\sqrt{B \cdot B(\rho = 0)}$ for $J_c(B)$ instead of Eq. (4).

The anisotropy of the upper critical magnetic field, γ, and the percolation parameter, p_c, were obtained from the best fits of Eq. (2) to the critical current density data, which are shown by solid curves in Fig. 1a, b for both the 600 and the 900 °C reaction temperatures, respectively. The results for the percolation parameter, p_c are plotted in Fig. 3. As can be seen in Fig. 3, the p_c increases with increasing temperature. This means that the number of connections between the grains decreases with increasing temperature. Therefore, the critical current density decreases with increasing temperature.

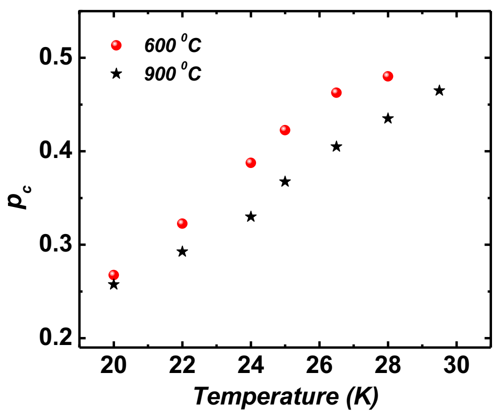

Fig. 3 Temperature dependence of the percolation threshold of the upper critical field for MgB_2 silicone oil-doped samples sintered at 600 and 900 °C

The values of the inferred anisotropy of the upper critical magnetic field, γ, are in agreement with previous reports [22]. It was found that the anisotropy of MgB_2 strongly depends on the purity of the material [25] and can change between about 6 in the clean limit and 1 in the dirty limit [22]. The anisotropy of MgB_2 decreases with increasing temperature as can be seen in Fig. 4.

The current transport in MgB_2 significantly alters the field dependence of the critical current density as shown in Fig. 1, and, consequently, of the volume pinning force, $F_p = J \times B$. The latter was recently used to derive information on the pinning mechanism in the same way as in isotropic or textured superconductors. Figure 5 shows the normalized volume pinning force, $f = F_p/F_{p,max}$, with $F_{p,max}$ the volume pinning force at the peak, as a function of reduced magnetic field, $b = B/B_{irr}$.

The position of the peak of the volume pinning force depends on the pinning centers, the anisotropy γ and the percolation threshold p_c. As can be seen in Fig. 5, the peak

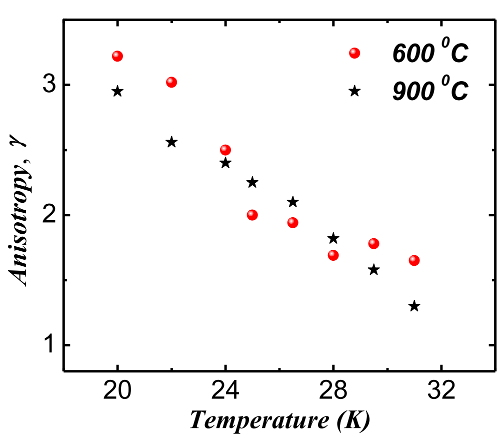

Fig. 4 Temperature dependence of the anisotropy of the upper critical field for MgB_2 silicone oil-doped samples sintered at 600 and 900 °C

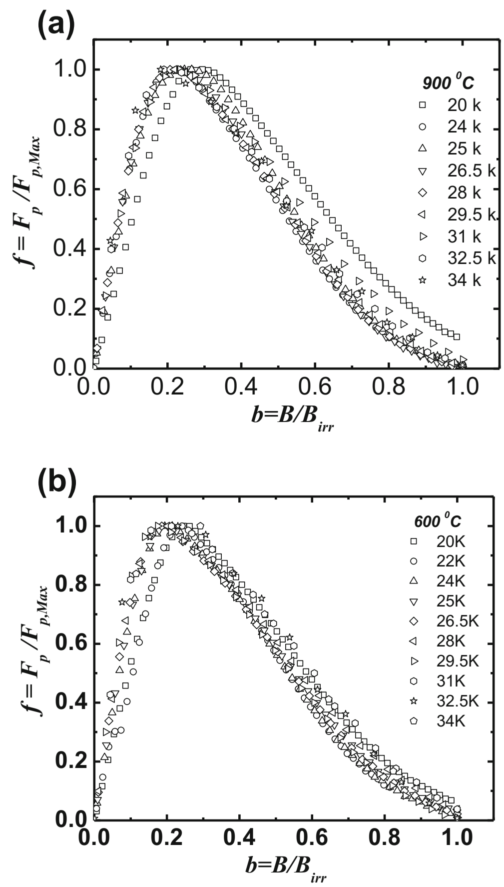

Fig. 5 Volume pinning force as a function of reduced magnetic field for two samples sintered at **a** 600 °C and **b** 900 °C

continuously shifts to lower reduced fields with decreasing anisotropy as the temperature increases. In the isotropic case, the peak position can be easily calculated from the power law $b^m(1-b)^n$ for the reduced pinning force f, which has its maximum at $m/(m+n)$. A value of 0.2 is obtained for grain boundary pinning ($m = 1/2$ and $n = 2$) [23].

The changes in F_p due to changes in the percolation threshold are comparatively small since the p_c variation is expected to be small in three-dimensional systems [4, 26]. Mainly, the number of connections between the grains determines the percolation threshold; thus, porous or dirty samples with a large amount of secondary phases have a comparatively large p_c and clean dense samples have a smaller p_c [22, 27]. As was shown in Fig. 3, the p_c increases with temperature which is supported by the shifts in the peak of the normalized volume pinning force to lower reduced field.

4 Conclusions

Increasing the sintering temperature improves the critical current of MgB_2 superconductor in the high magnetic field region, but does not change the trend of rapid reduction of the critical current density in high fields. This phenomenon can be explained by the anisotropy of the upper critical field based on the percolation model. The position of the peak of the volume pinning force depends on the pinning model, the anisotropy γ and the percolation threshold p_c. The position of the peak shifts to lower reduced magnetic field with decreasing anisotropy.

References

1. Nagamatsu, J., Nakagawa, N., Muranaka, T., Zenitali, Y., Akimitsu, J.: Nat. (Lond.) **410**, 63 (2001)
2. Kambara, M., Hari Babu, N., Sadki, E.S., Cooper, J.R., Minami, H., Cardwell, D.A., Campbell, A.M., Inoue, I.H.: Supercond. Sci. Technol. **14**, L5 (2001)
3. Finnemore, D.K., Ostenson, J.E., Bud'ko, S.L., Lapertot, G., Canfield, P.C.: Phys. Rev. Lett. **86**, 2420 (2001)
4. Eisterer, M., Zehetmayer, M., Weber, H.W.: Phys. Rev. Lett. **90**, 247002 (2003)
5. Christen, D.K., et al.: Mater. Res. Soc. Symp. Proc. **689**(E2), 1 (2002)
6. Kirkpatrick, S.: Rev. Mod. Phys. **45**, 574 (1973)
7. Davidson, A., Tinkham, M.: Phys. Rev. B **13**, 3261 (1976)
8. Deutscher, G., Entin-Wohlman, O., Fishman, S., Shapira, Y.: Phys. Rev. B **21**, 5041 (1980)
9. Entin-Wohlman, O., Kapitulnik, A., Alexander, S., Deutscher, G.: Phys. Rev. B **30**, 2617 (1984)
10. Specht, E.D., Goyal, A., Kroeger, D.M.: Phys. Rev. B **53**, 3585 (1996)
11. Prester, M.: Phys. Rev. B **54**, 606 (1996)
12. Osamura, K., Ogawa, K., Thamizavel, T., Sakai, A.: Phys. C **335**, 65 (2000)
13. Haslinger, R., JoyntR: Phys. Rev. B **61**, 4206 (2000)
14. Nakamura, Y., Izumi, T., Shiohara, Y.: Phys. C **371**, 275 (2002)
15. Zeimetz, B., Glowacki, B.A., Evetts, J.E.: Eur. Phys. J. B **29**, 359 (2002)
16. Tilley, D.R.: Proc. Phys. Soc. London **86**, 289 (1965)
17. Wang, X.L., Cheng, Z.X., Dou, S.X.: Appl. Phys. Lett. **90**, 042501 (2007)
18. Johansen T. H., Bratsberg H.: Phys. Rev. B **69**, 0125017 (2004)
19. Zhu, Y., Matsumoto, A., Senkowicz, B.J., Kumakura, H., Kitaguchi, H., Jewell, M.C., Hellstrom, E.E., Larbalestier, D.C., Voyles, P.M.: J. Appl. Phys **102**, 013913 (2007)
20. Kitaguchi, H., Matsumoto, A., Kumakura, H., Doi, T., Sosiati, H., Hata, S.: Appl. Phys. Lett. **85**, 2842 (2004)
21. Tilley, D.R.: Proc. Phys. Soc. **86**, 289 (1965)
22. Eisterer, M.: Supercond. Sci. Technol. **20**, R47 (2007)
23. Dew-Hughes, D.: Phil. Mag. **30**, 293 (1974)
24. Eisterer, M., Krutzler, C., Weber, H.W.: J. Appl. Phys. **98**, 033906 (2005)
25. Krutzler, C., Zehetmayer, M., Eisterer, M., Weber, H.W., Zhigadlo, N.D., Karpinski, J.: Phys. Rev. B **75**, 224510 (2007)
26. Van der Marck, S.C.: Phys. Rev. E **55**, 1514 (1997)
27. Eisterer, M., Schöppl, K.R., Weber, H.W., Sumption, M.D., Bhatia, M.: IEEE Trans. Appl. Supercond. **17**, 2814 (2007)